ARTICLE

Analysis of the LIF Spectroscopy of Nickel Hydride in 19000-21400 cm^{-1}

Jing-ru Guo, Ting-ting Wang, Zhao-xia Zhang, Cong-xiang Chen, Yang Chen*

Hefei National Laboratory for Physical Sciences at Microscale and Department of Chemical Physics, University of Science and Technology of China, Hefei 230026, China

(Dated: Received on February 26, 2008; Accepted on March 20, 2008)

The laser-induced fluorescence (LIF) excitation spectrum of NiH was recorded in the spectral region from 15000 cm^{-1} to 21400 cm^{-1}, with the NiH molecules produced by the reaction of sputtered nickel atoms with methanol under supersonic jet conditions. The 19000-21400 cm^{-1} portion of the spectrum of NiH is reported for the first time. Twenty-four bands were observed and classified into seven electronic transitions. Every band was rotationally analyzed. Higher vibrational levels of many excited states, A, B, D, E, F, and G, were observed and the complete set of spectroscopic parameters, vibrational frequency, unharmonic constant, rotational constant, and equilibrium length of these states were obtained. Some bands were reassigned.

Key words: NiH, Laser-induced fluorescence (LIF), Spectrum

I. INTRODUCTION

The electronic structure of nickel hydride attracts considerable interest due to its importance in astrophysics, organometallic chemistry, and surface science [1-3]. The optical spectrum of nickel hydride was first observed by Gaydon and Pearse in flames containing $Ni(CO)_4$ [4,5]. Two band systems subsequently designated as $A^2\Delta_{5/2}$-$X^2\Delta_{5/2}$ and $B^2\Delta_{5/2}$-$X^2\Delta_{5/2}$ were reported. Heimer photographed absorption spectrum of NiH by heating nickel metal in hydrogen atmosphere in a King furnace [6]. Two more bands of the $B^2\Delta_{5/2}$-$X^2\Delta_{5/2}$ transition were discovered, and also two violet bands assigned to the $C^2\Delta_{5/2}$-$X^2\Delta_{5/2}$ transition. Åslund *et al.* rephotographed the violet system and identified two subsystem $C^2\Delta_{3/2}$-$X^2\Delta_{3/2}$ and $C^2\Delta_{3/2}$-$X^2\Delta_{5/2}$ [7]. The results indicated that the ground state of NiH is an inverted $^2\Delta$ state with large spin-orbit splitting (A=−490 cm^{-1}). In later work, Scullman and coworkers investigated the emission spectrum of NiH as well as NiD with a hollow cathode source [8,9]. Three electronic states, named $D1.5$, $F3.5$, and $I1.5$, were reported. Considerable progress in the visible spectrum analysis was possible thanks to the cooperative work of the Stockholm group and the MIT group [10,11]. Both grating spectrograph and laser-induced fluorescence spectrum of NiH and NiD have been recorded. All transitions in the 15500-19000 cm^{-1} have been carefully analyzed. The $E1.5$, $I1.5$, and $G2.5$ states were discovered and some formerly reported bands were reassigned. Field *et al.* also studied the Stark and Zeeman effects of NiH and used the results to demonstrate the assignment of the electronic states [12-14]. A supermultiplet model was founded thereafter to improve the explanation of the electronic structure of the transition metal monohydride molecule [15,16]. Except for the $C^2\Delta$ state, all the reported excited states of NiH were located in the visible region.

The low-lying states of NiH have also been studied in detail. The ground state was identified as $X^2\Delta$ sate from the $1\sigma^2 2\sigma^2 1\delta^3 1\pi^4$ configuration. The infrared and far-infrared spectra of NiH as well as NiD have been detected using laser magnetic resonance by Nelis *et al.* [17-20]. The vibrational, rotational and hyperfine structure of the ground state has been analyzed. The accurate spin-orbit coupling constant, the vibrational frequency, the rotational constant and the equilibrium bond length were determined.

Many quantum chemistry studies have attempted to predict the energy order of the low-lying states of NiH [21-23]. The bond length, dissociation energy and dipole moment of the ground state have been calculated.

In this work we reinvestigated the LIF excitation spectroscopy of NiH molecules. The spectral region was extended to 21400 cm^{-1}. The wider wavelength coverage spectra allowed high vibrational levels of the previously reported state transitions to be observed. Therefore more precise information of the excited states of NiH could be obtained and the molecular parameters of those states could be improved.

II. EXPERIMENTS

The gas-phase NiH molecules were produced by the reaction of sputtered nickel atoms with methanol under discharge condition. Their spectra were recorded by laser-induced fluorescence (LIF) under supersonic jet-cooled conditions.

The experimental apparatus has been described in the previous publications of our laboratory in detail [24,25] and will be outlined here briefly. A couple of nickel pins were used as electrodes for DC discharge.

*Author to whom correspondence should be addressed. E-mail: yangchen@ustc.edu.cn, Tel: +86-551-3606619

The supplied voltage was approximately 2 kV. The sputtered nickel atoms reacted with a pulse of saturated methanol vapor in argon carrier gas at a backing pressure of 606 kPa. The products expanded into the vacuum chamber, where the average working pressure was 40 mPa, formed a supersonic molecular beam. A pulsed dye laser (Lumonics: HD-500) pumped by a Nd:YAG laser (Spectra Physics: GCR-170) was used as the probe laser. The dye laser (with a linewidth of 0.1 cm^{-1} and a pulse width of 5 ns) crossed the molecular beam 3 cm downstream from the point of discharge. The excited fluorescence was collected by a set of lenses and finally recorded by a photomultiplier tube (Hamamatsu R928). The signal was amplified, averaged, integrated and sent to the computer. The laser-induced fluorescence was collected orthogonal to both the molecular beam and the probe laser. The operation of the nozzle, the discharge and the laser pulse were controlled sequentially by a multi-channel pulse generator. The laser dyes used were LDS 698, DCM, Kiton Red 620, Rhodamine 590, Coumarin 540A, Coumarin 503, and Coumarin 480. All of them were products of Exciton Inc. The laser wavelength was calibrated by optogalvanically active argon lines.

III. RESULTS AND DISCUSSION

The LIF excited spectrum of NiH under supersonic jet-cooled conditions was recorded in the wavelength range 470-730 nm. A total of twenty-four bands were observed. Eight of them were previously undiscovered. This wide range spectrum took several weeks to complete. For the convenience of discussion, the whole spectrum will be divided into three parts. (i) The spectrum in the 15000-19000 cm^{-1} region has been fully investigated. Most of the previously reported transition bands were in this region [4-6,8-11]. We did not find any new bands here and our analysis results are in agreement with the previous work. (ii) The spectrum in the 19000-20200 cm^{-1} region was crowded. Transitions from the ground state to high vibrational energy levels of many states were observed. (iii) In the range 20200-21400 cm^{-1}, the spectroscopic intensity markedly weakened, while the spectrum became more complicated. Since the dissociation limits of many excited states of NiH are located in this region, the upper states of the transitions were predicted to be predissociated.

Under our supersonic jet-cooled conditions, all the transitions arose from the ground state $X^2\Delta_{5/2}$ (v=0) level. The bands of NiH were strongly red-degraded with the R branch forming a band head. The intensity of every branch decreased rapidly with increasing J. With low rotational temperature and large rotational constants, the number of J value observed in an NiH band was usually no more than ten. Also we found extremely large Λ-doubling in some bands. Except for the (0,0) band, there were isotopic shifts of the band lines due to the other isotopomers of NiH. There were five nickel isotopes with abundance ^{58}Ni, 68.27%; ^{60}Ni, 26.10%; ^{61}Ni, 1.13%; ^{62}Ni, 3.59%; and ^{64}Ni, 0.91%. The intensity distribution of the band lines was in the same proportion. The magnitude of the isotopic shifts was good evidence to determine the vibrational number of the upper state. The expressions of the transition energies for the ^{58}Ni^{1}H and ^{60}Ni^{1}H were given by:

$$T'_v(^{58}\mathrm{Ni}^1\mathrm{H})=T_e+\omega'_e\left(v'+\frac{1}{2}\right)-\omega''_e\left(v''+\frac{1}{2}\right) \quad (1)$$

$$T'_v(^{60}\mathrm{Ni}^1\mathrm{H})=T_e+\rho\omega'_e\left(v'+\frac{1}{2}\right)-\rho\omega''_e\left(v''+\frac{1}{2}\right) \quad (2)$$

where ρ was given by

$$\rho=\sqrt{\frac{\mu(^{58}\mathrm{Ni}^1\mathrm{H})}{\mu(^{60}\mathrm{Ni}^1\mathrm{H})}}=0.9997 \quad (3)$$

The isotopic shift is

$$\begin{aligned}\Delta\nu &= T'_v(^{60}\mathrm{Ni}^1\mathrm{H})-T'_v(^{58}\mathrm{Ni}^1\mathrm{H})\\ &= (1-\rho)\left[\omega'_e\left(v'+\frac{1}{2}\right)-\omega''_e\left(v''+\frac{1}{2}\right)\right]\end{aligned} \quad (4)$$

The Ω number of the state was decided by the lowest J line of the P, Q, and R branch.

Since the designation of some excited states of NiH are still under dispute, here we name all the bands with the empirical notation $[T_v]\Omega'$, where T_v is the band origin in thousands of wavenumbers. All of the bands observed in this work were fitted to the empirical expression

$$E(J)=T_v+B_{\mathrm{eff}}J(J+1)-D_{\mathrm{eff}}J^2(J+1)^2 \quad (5)$$

The results are listed in Table I.

With the constants obtained by the fitting, we calculated the equilibrium constants for all the upper electronic states, using the expressions

$$T_v = T_e+\omega_e\left(v+\frac{1}{2}\right)-\omega_e\chi_e\left(v+\frac{1}{2}\right)^2 \quad (6)$$

$$B_v = B_e-\alpha_e\left(v+\frac{1}{2}\right) \quad (7)$$

The results are listed in Table II.

A. The $A2.5$-$X_1 2.5$ transition

The A2.5 state was first assigned as $^2\Delta_{5/2}$, while the later Zeeman effect observation suggests $^4\Phi_{5/2}$ character [11]. The (0,0) band of the $A2.5$-$X_1 2.5$ transition was identified by Gaydon and Pearse in 1935 [5]. In later work [8,11], the (1,0) and (2,0) bands were analyzed. The analysis now has been increased with the

DOI:10.1088/1674-0068/21/04/308-313

TABLE I Molecular constants for the assigned bands of NiH (in cm^{-1}).

State	v	T_v	$B_v^{\rm eff}$	$D_v^{\rm eff}\times10^{-4}$
$A2.5$	$4^{a,b}$	20945.1(2)	4.75	0
	3^{a}	19760.10	5.429	7
	2	18450.7	5.761(3)	3.3
	1	17036.06	6.021(1.5)	4.6
	0	15528.2(3)	6.277	4
$B2.5$	3	20164.8(2)	5.788(2)	20
	2^{b}	18878.6(7)	5.52	0
	1^{b}	17482.2	5.42	3.4
	0^{b}	15985.3(10)	5.38	0
$D1.5$	$3^{a,b}$	20418.6(8)	5.69	33
	2^{a}	19106.3(1)	5.817(15)	15
	1	17680.7(1)	6.238(3)	8
	0	16157.9(3)	6.596(3)	17
$E1.5$	$3^{a,b}$	20591.1(1)	4.74(1)	0
	2^{a}	19272.7(2)	5.502(2)	13.6
	1	17861.2(2)	5.791(6)	0.8
	0	16346.1(2)	6.217(2)	5.4
$F3.5$	2^{a}	19847.9	5.567	0
	1	18530.4(1)	6.020	4.7
	0	17100.7	6.297	0
$G2.5$	1^{a}	19869.3(1)	6.060	10
	0	18437.9(7)	6.263	0
$I1.5$	1	18752.9	5.357	10
	0	17317.3	5.818	7.6

[a] New states observed in this work.
[b] States too perturbed to allow a sensible rotational fit. The rotational constants were only approximate. For the other states, the RMS error of the fit was less than 0.3. The lower state constants for fitting were set to the value of Ref.[8], B_v''=7.7005 cm^{-1}, $D_v''=4.82\times10^{-4}$ cm^{-1}. Constants were given for the main isotope ^{58}NiH. For the $B2.5$ (v=3) and $D1.5$ (v=1) state, only the strongest components of the splitting was fitted.

(3,0) and (4,0) bands. These two bands were $A[19.7]2.5$-$X_12.5(3,0)$ at 505.6 nm and $A[20.9]2.5$-$X_12.5$ (4,0) at 477.4 nm. The wavenumbers of the band lines are listed in Table III. The intensity patterns of those two bands are like the others, that is, a reasonably strong R branch, a slightly weaker P branch, and an intense Q branch, with the first Q line, Q(2.5), being the strongest in the whole band. The v=3 and v=4 energy levels of the $A2.5$ state were relatively unperturbed.

B. The $B2.5$-$X_12.5$ transition

The $B2.5$-$X_12.5$ transition system was the strongest in our visible spectra. All the four bands (0,0), (1,0), (2,0), and (3,0) were known earlier [6]. Strong perturbation can be seen in every band. We found that the rotational structure of the $B[20.2]2.5$-$X_12.5(3,0)$ band is extremely complicated. Every rotational line was split into three components; the most intense line situated in the middle, a weak line with about half the intensity situated to the red of the main line and a strong line situated to the blue. Isotopic shifts in the three components were slightly different, too. -doubling can be found only in the Q(2.5) line. This band was reassigned. See Table III. Clearly, the upper state of the $B2.5$-$X_12.5$ transition was perturbed. See Fig.1.

C. The $D1.5$-$X_12.5$ transition

The $D[17.6]1.5$-$X_12.5(1,0)$ band was first reported in Ref.[11], where it was described as double R, Q, and P branches. Actually we found that the structure of this band has similar appearance to the $B[20.2]2.5$-$X_12.5(3,0)$ band. Every rotational line was split into three. The only difference was the intensity order of the three components. In this case, the weak line was located in the blue spectral region and the strong line in the red, with the most intense one still in the middle. The wavenumbers of the band lines are listed in Table III.

Two bands at 522.7 and 489.7 nm were assigned as the (2,0) and (3,0) bands of the $D1.5$-$X_12.5$ transition, respectively. The (2,0) band was pretty strong and the (3,0) band fairly weak. The bands featured a strong Q branch and slightly weak R and P branch, and the intensity of the P branch decreased rapidly with increasing J. Very large Λ-doubling was still a notable characteristic of the D1.5 rotational energy level. In these two bands the magnitude of Λ-doubling splitting was not as large as for the (0,0) and (1,0) bands. The $D1.5$ (v=3) state was too perturbed to allow a sensible rotational fit. See Fig.1.

D. The $E1.5$-$X_12.5$ transition

Four bands of the $E1.5$-$X_12.5$ transition were recorded. Of these, the (2,0) and (3,0) bands were observed for the first time. The intensity feature of the $E1.5$-$X_12.5$ transition bands was similar to that of the $D1.5$-$X_12.5$ transition bands. The (2,0) band at 518.8 nm of the E1.5-$X_1$2.5 transition was strong whereas the (3,0) band at 475.4 nm was very weak. The appearance of the $E1.5$-$X_12.5$ transition bands were like those of the $D1.5$-$X_12.5$ transition bands, too. As for the rotational level, there was also extremely large Λ-doubling in all vibrational levels of the $E1.5$ state. The $E1.5$ v=3 level was a severely perturbed state.

E. The $F3.5$-$X_12.5$ transition

The F state was the only reported Ω=3.5 state of NiH. For all the $F3.5$-$X_12.5$ transition bands, the R branch was strong, the Q branch was slightly weak, and

DOI:10.1088/1674-0068/21/04/308-313

TABLE II Equilibrium constants for the excited state of NiH (in cm^{-1}).

State	T_e	ω_e	$\omega_e\chi_e$	B_e	α_e	R_e/Å
$A2.5$	14726(10)	1624(10)	54(2)	6.56(13)	0.36(5)	1.611
$B2.5$	15196(4)	1604(4)	53(1)	5.26(8)	−0.13(3)	1.799
$D2.5$	15354(6)	1631(7)	53(2)	6.80(3)	0.39(2)	1.582
$E2.5$	15553(4)	1611(5)	49(1)	6.51(15)	0.47(7)	1.617
$F3.5$	16344	1542	56	6.51(8)	0.37(5)	1.617
$G2.5$	18438[a]	1431[b]				
$I2.5$	17317[a]	1436[b]				

[a] T_0 value.
[b] $\Delta G_{1/2}$ value.

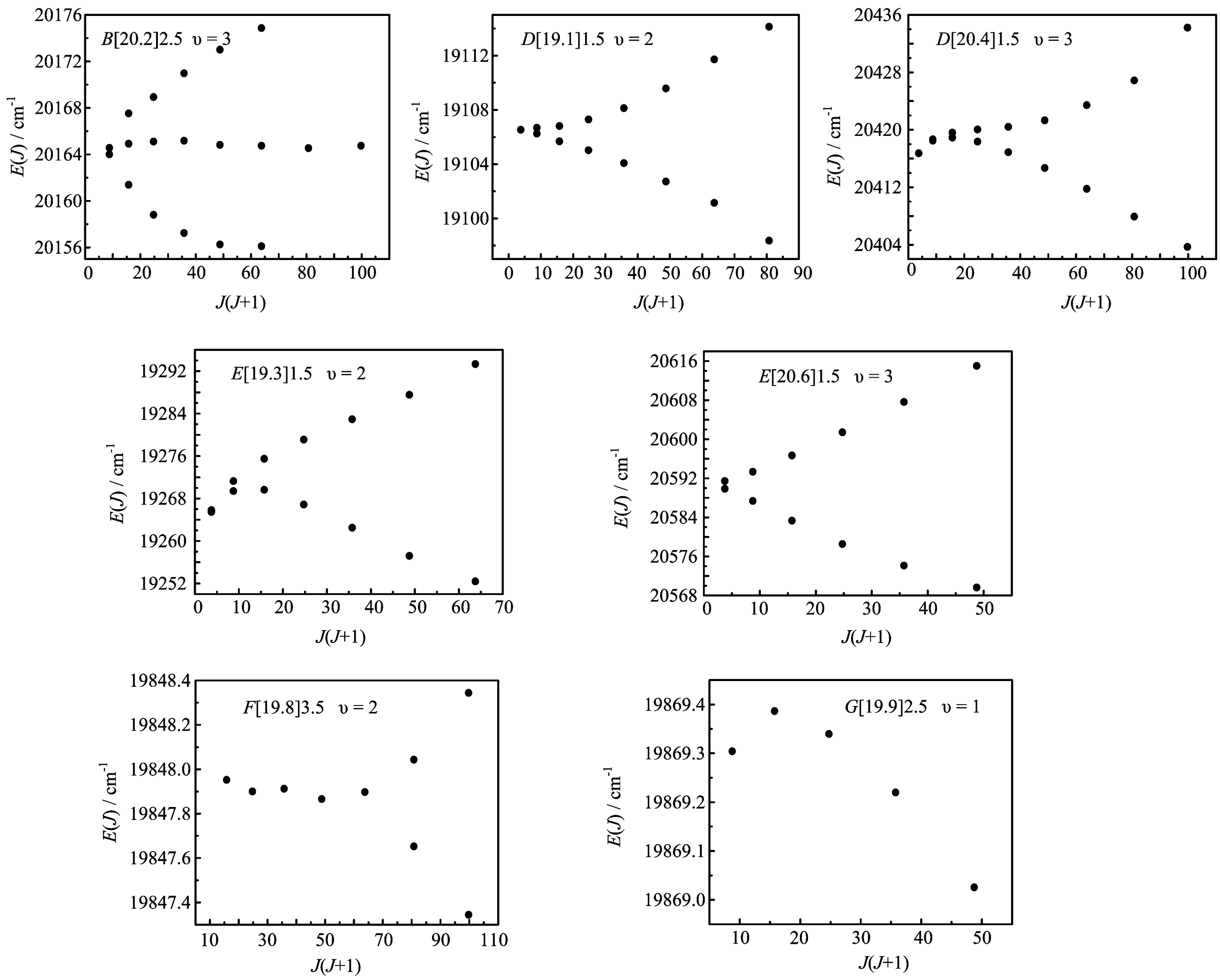

FIG. 1 Reduced energy plot for some perturbed new observed bands of NiH as a function of $J(J+1)$, a term $B_{\mathrm{eff}}J(J+1)-D_{\mathrm{eff}}J^2(J+1)^2$ has been subtracted to expand the scale.

no P branch was observed. Guided by the 0.65 cm^{-1} isotopic shift of v'=2, the (2,0) band of the $F3.5$-$X_12.5$ transition was discovered at 503.8 nm. The wavenumbers of the band lines are listed in Table III.

F. The $G2.5$-$X_12.5$ transition

The G state was first discovered in Ref.[11], where the (0,0) band was analyzed. In the present work, the (1,0) band of the $G2.5$-$X_12.5$ transition was discovered

DOI:10.1088/1674-0068/21/04/308-313

TABLE III Rotational line positions for the new observed bands of NiH (cm^{-1}). All lines are given for the main isotope ^{58}NiH.

J	A[19.7]2.5-$X_1$2.5 (3,0)			A[20.9]2.5-$X_1$2.5 (4,0)			G[19.9]2.5-$X_1$2.5 (1,0)			F[19.8]3.5-$X_1$2.5 (2, 0)		
	R	Q	P	R	Q	P	R	Q	P	R_e	R_f	Q
2.5	19778.07	19740.19		20952.96	20919.22		19897.44	19854.91	19868.29			
3.5	19772.85	19724.25	19686.42	20941.30	20899.13	20865.38	19897.80	19843.42	19800.94	19864.52		19814.43
4.5	19762.98	19703.80	19655.17	20925.14	20872.05	20830.07	19894.54	19828.42	19774.19	19856.64		19795.23
5.5	19748.40	19678.66	19619.37			20787.85	19887.65	19809.91	19743.90	19844.58		19772.15
6.5	19729.02	19649.07	19578.78					19787.82	19710.36	19828.54		19744.93
7.5			19532.67							19808.63	19808.24	
8.5										19784.98	19783.98	

J	B[20.2]2.5-$X_1$2.5(3, 0)								
	R			Q			P		
2.5	20190.97	20188.35	20184.87		20147.72	20147.16			
3.5	20189.99	20186.16	20179.84	20137.03	20134.42	20130.89		20093.84	20093.28
4.5	20185.19	20179.37	20171.43	20120.67	20116.84	20110.54	20067.68	20065.08	20061.60
5.5	20175.94	20167.76	20159.18	20100.67	20094.87	20086.93	20036.12	20032.28	20025.98
6.5	20161.48	20151.36	20142.72	20076.17	20067.99	20059.42	20001.08	19995.27	19987.33
7.5		20129.94					19961.50	19953.48	19944.89
8.5		20103.55					19917.07	19907.03	19898.29
9.5		20071.87							
	D[17.6]1.5-$X_1$2.5(1,0)								
2.5	17708.57	17711.34	17714.84	17665.57	17667.94	17670.35	17635.87	17636.97	17639.09
3.5	17710.16	17713.31		17654.64	17657.43	17660.92	17611.65	17614.00	17616.43
4.5	17707.89	17712.32		17640.92	17644.02				
5.5	17701.52	17708.29		17623.40	17627.83				
6.5	17690.94	17701.06		17601.78	17608.46				
7.5	17676.77	17690.57							
8.5		17675.96							

	J	R_e	R_f	Q_{ef}	Q_{fe}	P_e	P_f
D[19.1]1.5-$X_1$2.5(2,0)	2.5	19131.02	19129.91	19090.12	19089.69	19060.80	
	3.5	19129.49	19127.25	19076.89	19075.76	19036.08	19035.66
	4.5	19124.17	19120.12	19060.05	19057.78	19007.60	19006.51
	5.5	19115.08	19108.36	19039.49	19035.44		
	6.5	19102.20	19091.62	19015.34	19008.47		
	7.5	19085.11	19069.35				
D[20.4]1.5-$X_1$2.5 (3,0)	2.5	20441.06	20440.37	20400.92	20400.71	20370.69	
	3.5	20437.69	20436.00	20387.31	20386.61	20347.05	20346.86
	4.5	20429.32	20425.78	20368.48	20366.79		
	5.5	20416.19	20409.55	20344.97	20341.47		
	6.5	20398.50	20386.86				
	7.5	20375.87	20356.91				
	8.5	20350.30	20319.77				
E[19.3]1.5-$X_1$2.5 (2,0)	2.5	19294.49	19288.66	19252.12	19250.20	19219.10	19218.75
	3.5	19293.27	19281.05	19240.66	19234.86	19198.16	19196.27
	4.5	19287.60	19267.18	19224.18	19211.95	19171.52	19165.68
	5.5	19277.84	19247.50	19203.11	19182.67		
	6.5	19264.30	19223.36	19178.28	19147.90		
E[20.6]1.5-$X_1$2.5 (3,0)	2.5	20603.98	20590.64	20567.49	20561.52	20541.88	20540.28
	3.5	20597.58	20574.70	20550.26	20536.97	20513.66	20507.67
	4.5	20586.78	20553.28	20528.58	20505.56	20481.07	20467.70
	5.5	20571.4	20526.05	20502.37	20468.81		

DOI:10.1088/1674-0068/21/04/308-313

at 503.3 nm. It is a parallel transition band with strong R and Q branch, and the P branch somewhat less intense. No Λ-doubling was discovered under the J value observed. It was not certain that the $G2.5$-$X_12.5$ progression died out at v=1 because a band fragment with isotopic shift 0.65 cm^{-1} at 21200 cm^{-1} was discovered, which was situated exactly in the predicted energy region of the $G2.5$-$X_12.5$ (2,0).

G. The $I1.5$-$X_1 2.5$ transition

No new bands could be assigned to the $I1.5$-$X_12.5$ transition. Only the v'=0 and v'=1 vibrational levels were observed. The $I1.5$ state was predicted to have a shallow potential well in which the dissociation limit was below the v'=2 level. We have noticed that the rotational constants of the $I1.5$ state were less than the other states, as shown in Table I, so the equilibrium bond length of the $I1.5$ state must be a little longer.

In general, the transition metal monohydrides and monohalides (particularly monofluorides) were very similar in energy levels. However, this was not the case for NiH and nickel monohalides since these two kinds of molecules had intricate perturbation systems. There were three low lying states for all of them, but the energy order was different, for NiH, the $^2\Delta$ state is the lowest, while NiF and NiCl have $^2\Pi$ ground state. As for the excited states, both NiH and NiF have eight electronic states observed in the 15000-24000 cm^{-1} range [26], the two set of states were quite different not only in energy order, but also in their symmetries.

Our spectral range 15000-21400 cm^{-1} includes the richest information for the upper states of NiH. In the higher energy range, NiH bands are predissociated. The dissociation energies (D_e value) for the ground state of the three iron peak elements hydrides, FeH, CoH, and NiH, are 3.2, 1.9, and 2.6 eV, respectively [27]. Only FeH has spectra higher than 22000 cm^{-1}.

IV. CONCLUSION

NiH molecules were produced by DC discharge of nickel electrodes with methanol. Laser induced fluorescence excitation spectra were taken under super sonic free jet conditions. The spectral range was extended to 15000-21400 cm^{-1}. In the 19000-21400 cm^{-1} spectra of NiH, the high vibrational levels of the A, B, D, E, F, and G state transition bands were observed and analyzed. A complete set of spectroscopic parameters of these states was obtained.

V. ACKNOWLEDGMENTS

This work was supported by the National Natural Science Foundation of China (No.20433080), the Chinese National Key Basic Research Special Foundation (No.G1999075304), and the Chinese Academy of Science (No.KJCX2-SW-H08).

[1] D. L. Lambert and E. A. Mallia, Mon. Not. R. Astron. Soc. London **151**, 437 (1971).
[2] T. M. Upton, J. Am. Chem. Soc. **106**, 1561 (1984).
[3] P. E. M. Siegbahn, M. R. A. Blomberg, I. Panas, and U. Wahlgern, Theor. Chim. Acta **75**, 143 (1984).
[4] A. G. Gaydon and R. W. Pearse, Nature **134**, 287 (1934).
[5] A. G. Gaydon and R. W. Pearse, Proc. R. Soc. A **148**, 312 (1935).
[6] A. Heimer, Z. Phys. **105**, 56 (1937).
[7] N. Åslund, H. Neuhaus, A. Lagerqvist, and E. Andersen, Ark. Fys. **28**, 271 (1964).
[8] R. Scullman, S. Löfgren, and S. A. Kadavathu, Phys. Scr. **25**, 295 (1982).
[9] S. A. Kadavathu, S. Löfgren, and R. Scullman, Phys. Scr. **35**, 277 (1987).
[10] S. A. Kadavathu, R. Scullman, J. A. Gray, M. Li, and R. W. Field, J. Mol. Spectrosc. **140**, 126 (1990).
[11] S. A. Kadavathu, R. Scullman, R. W. Field, J. A. Gray, and M. Li, J. Mol. Spectrosc. **147**, 448 (1991).
[12] J. A. Gray, S. F. Rice, and R. W. Field, J. Chem. Phys. **82**, 4717 (1985).
[13] J. A. Gray and R. W. Field, J. Chem. Phys. **84**, 1041 (1986).
[14] M. Li, J. A. Gray, and R. W. Field, Chem. Phys. **117**, 171 (1987).
[15] J. A. Gray, M. Li, and R. W. Field, J. Chem. Phys. **92**, 4651 (1990).
[16] J. A. Gray, M. Li, T. Nelis, and R. W. Field, J. Chem. Phys. **95**, 7164 (1991).
[17] T. Nelis, E. Bachem, W. Bohle, and W. Urban, Mol. Phys. **64**, 7595 (1988).
[18] S. P. Beaton, K. M. Evenson, T. Nelis, and J. M. Brown, J. Chem. Phys. **89**, 4446 (1988).
[19] K. Lipus, U. Simon, E. Bachem, T. Nelis, and W. Urban, Mol. Phys. **67**, 1431 (1989).
[20] T. Nelis, S. P. Beaton, and K. M. Evenson, J. Mol. Spectrosc. **148**, 462 (1991).
[21] C. M. Rohlfing, P. J. Hay, and R. L. Martin, J. Chem. Phys. **85**, 1447 (1986).
[22] C. M. Marian, M. R. A. Blomberg, and P. E. M. Siegbahn, J. Chem. Phys. **91**, 3589 (1989).
[23] C. M. Marian, J. Chem. Phys. **93**, 1176 (1990).
[24] Y. Chen, J. Jin, C. J. Hu, X. L. Yang, X. X. Ma, and C. X. Chen, J. Mol. Spectrosc. **203**, 37 (2000).
[25] J. Jin, Q. Ran, X. L. Yang, Y. Chen, and C. X. Chen, J. Phys. Chem. A **105**, 11177 (2001).
[26] Y. Krouti, T. Hirao, C. Dufour, A. Boulezhar, B. Pinchemel, and P. F. Bernath, J. Mol. Spectrosc. **214**, 152 (2002).
[27] M. C. McCarthy and R. W. Field, J. Chem. Phys. **100**, 6347 (1994).

DOI:10.1088/1674-0068/21/04/308-313